

Mixed-ligand copper(I) halide complexes bearing 4,5-bis(diphenylphosphano)-9,9-dimethyl-xanthene and *N*-methylbenzothiazole-2-thione: Synthesis, structures, luminescence and antibacterial activity mediated by DNA and membrane damage

O. Evangelinou^a, A.G. Hatzidimitriou^a, E. Velali^b, A.A. Pantazaki^{b,*}, N. Voulgarakis^c, P. Aslanidis^{a,*}

^a Laboratory of Inorganic Chemistry, Department of Chemistry, Aristotle University of Thessaloniki, GR-541 24 Thessaloniki, Greece

^b Laboratory of Biochemistry, Department of Chemistry, Aristotle University of Thessaloniki, GR-541 24 Thessaloniki, Greece

^c Department of Logistics, Alexander Technological Educational Institute of Thessaloniki, GR-60100 Katerini, Greece

ARTICLE INFO

Article history:

Received 18 November 2013

Accepted 2 February 2014

Available online 11 February 2014

Keywords:

Copper(I)

N-Methylbenzothiazole-2-thione

Luminescence

Crystal structures

Antimicrobial activity

DNA interaction

Reactive oxygen species (ROS)

ABSTRACT

The 1:1 M-ratio reaction between copper(I) bromide or iodide and 4,5-bis(diphenylphosphano)-9,9-dimethyl-xanthene (xantphos) in acetonitrile results in the formation of $[\text{CuX}(\text{xantphos})]$ ($\text{X} = \text{Br}, \text{I}$), which further reacts with *N*-methylbenzothiazole-2-thione (mbtt) to afford the mononuclear mixed-ligand complexes $[\text{CuX}(\text{xantphos})(\text{mbtt})]$. The molecular structures of the complexes, established by single-crystal X-ray diffraction, feature a distorted tetrahedral geometry around the metal center, with the diphosphane acting as a chelate. The new compounds are strongly emissive in the solid state at room temperature. The complexes were also screened for antibacterial activity and their ability to interact with CT-DNA *in vitro* and to produce reactive oxygen species (ROS).

© 2014 Elsevier Ltd. All rights reserved.

1. Introduction

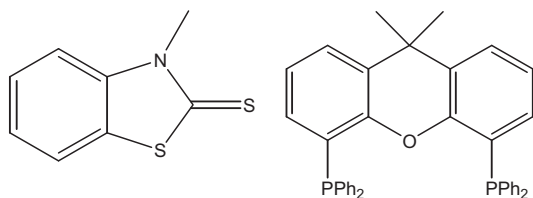
Owing to the favourable soft acid–soft base interaction, the chemistry of the univalent coinage metal ions is largely based upon coordination by ligands containing P and/or S donor atoms. A vast amount of copper(I) and silver(I) complexes with tertiary phosphanes as ligands has been accumulated over the years, many of which were employed in catalytic processes [1–3], while some of them were even found to exhibit antitumor activity [4]. As for the S-donor ligands, substantial interest has been given to the extended family of heterocyclic thiones, which are regarded as a very promising starting point for biological studies because of their close structural resemblance to thioamides, and due to the fact that many thione-ligated metal complexes are known to have relevance to biological systems [5–7]. In this respect, several imidazole-, thiazole-, thiadiazole-, oxazole-, uracil- and hydantoin-based thioamide derivatives as well as their transition metal complexes have

been tested in recent years towards pharmacological activities, such as antiviral, antibacterial or antifungal [8–13].

Based on the rich coordination chemistry produced so far for each of these two classes of ligands, we have long been engaged in the investigation of mixed-ligand copper(I) and silver(I) complexes bearing both bulky triaryl phosphanes and heterocyclic thione ligands aiming to gain insight into the interplay between the ligand's characteristics and the structural diversity observed [14]. In addition, having recognized that current interest in copper complexes largely focuses on their potential use as antimicrobial, antiviral, anti-inflammatory and antitumor agents, we recently turned our attention to the biochemical properties of these compounds, reporting the synthesis and characterization of copper(I) halide complexes of *N*-methylbenzothiazole-2-thione (mbtt, Scheme 1) from type $[\text{CuX}(\text{mbtt})_2]$ and $[\text{CuX}(\text{mbtt})(\text{PPh}_3)_2]$ and investigating their antibacterial activity and their interaction with CT-dsDNA [15]. Note that the vast majority of the hitherto tested copper-based compounds are copper(II) complexes, whereas respective studies on the copper(I) ones are relatively few and essentially limited to derivatives bearing ligands capable of stabilizing the low oxidation state of the metal ion in aqueous media [16,17]. On the ground of our very promising findings, and because of the fact that

* Corresponding authors.

E-mail addresses: natasa@chem.auth.gr (A.A. Pantazaki), aslanidi@chem.auth.gr (P. Aslanidis).



Scheme 1. The heterocyclic thione *N*-methylbenzothiazole-2-thione (mbtt) and the diphosphane 4,5-bis(diphenylphosphano)-9,9-dimethyl-xanthene (xantphos) used as ligands.

perceptibly stronger antibacterial activity was found for the derivatives bearing the triphenylphosphane co-ligand, we decided to further extend our studies considering bidentate P-donor ligands with an already established chelating behavior towards copper(I). According to our hitherto experience with the use of such arylphosphanes in the synthesis of mixed-ligand copper(I) halide complexes bearing heterocyclic thiones, 4,5-bis(diphenylphosphano)-9,9-dimethyl-xanthene (xantphos, Scheme 1), despite of its more or less configurationally inflexible heteroarene skeleton, proved to be best designed to chelate to copper(I) and silver(I) both in a tetrahedral or trigonal coordination environment, with the coordination number apparently being determined by the nature of the co-ligands present. In particular, the synthesis and characterization of some tetrahedral complexes of the general formula [CuBr(xantphos)(thione)] obtained by the treatment of a CuBr/xantphos intermediate with some neutral heterocyclic thioamides was reported some years ago [18]. More recently we were able to isolate and structurally characterize [AgBr(xantphos)] as a monomer with a roughly trigonal environment around the metal centre, which has been further used as an intermediate for the synthesis of tetrahedrally coordinated mixed-ligand complexes of type [AgBr(xantphos)(thione)] [19].

In this work we present two new luminescent copper(I) complexes of type [CuX(xantphos)(mbtt)] and investigate their antibacterial activity, the *in vitro* CT-dsDNA damage and the levels of lipid peroxidation.

It is known that in aerobic microorganisms, the respiration process has the inevitable downside of electron leakage from redox enzymes to oxygen, forming reactive oxygen species (ROS) such as hydrogen peroxide (H₂O₂), the superoxide radical (O₂^{•−}), and the hydroxyl radical (OH[•]). ROS accumulation results many biological effects among them lipid peroxidation, and DNA damage [20,21]. Thus, to investigate the antibacterial mechanism, we have measured the generation of reactive oxygen species (ROS) in the presence of these complexes measured as MDA equivalents and we have examined the *in vitro* DNA damage in agarose gel electrophoresis.

2. Experimental

2.1. Materials and instrumentation

Commercially available copper(I) bromide and iodide (Merck) and 9,9-dimethyl-4,5-bis(diphenylphosphano)xanthene (Aldrich) were used as received while *N*-methylbenzothiazole-2-thione (Aldrich) was re-crystallized from hot ethanol prior to its use. All solvents were purified by respective suitable methods and allowed to stand over molecular sieves. Infra-red spectra in the region of 4000–200 cm^{−1} were obtained in KBr discs with a Nicolet FT-IR 6700 spectrophotometer, while a Shimadzu 160A spectrophotometer and a Hitachi F-7000 fluorescence spectrometer were used to obtain the electronic absorption (UV–Vis) and emission/excitation spectra respectively. Melting points of the compounds were

measured in open tubes with a STUART scientific instrument and are uncorrected.

2.2. Crystal structure determination

Single crystals of [CuBr(xantphos)(mbtt)] (**1**) and [CuI(xantphos)(mbtt)] (**2**) suitable for crystal structure analysis were obtained by slow evaporation of their mother liquids at room temperature. Both crystals were taken from their mother liquor, mounted in air and covered with epoxy glue. Diffraction measurements were made on a Bruker Kappa APEX II diffractometer equipped with a triumph monochromator. Data collection (ϕ and ω -scans) as well as processing (cell refinement, data reduction and numerical absorption correction) were performed using the APEX2 program package [22]. The structures were solved using SUPERFLIP program [23] and refined by full-matrix least-squares methods on F^2 using the CRYSTALS program package [24]. In both structures, all non-hydrogen atoms were refined anisotropically. Hydrogen atoms were either located by difference maps or were introduced at calculated positions as riding on bonded atoms. Further crystallographic details are summarized in Table 1. Details on the crystallographic studies as well as atomic displacement parameters are given as Supporting Information in the form of cif files. Illustrations were generated using the CAMERON program [25].

2.3. Synthesis of compounds **1** and **2**

A suspension of 0.5 mmol of copper(I) halide (49.5 mg for CuCl, 72 mg for CuBr, 95 mg for CuI) in 50 mL of dry acetonitrile was stirred to give a clear solution which was then treated with solid 4,5-bis(diphenylphosphano)-9,9-dimethyl-xanthene (289.3 mg, 0.5 mmol) added in small portions. After stirring for two hours at 50 °C, a solution of *N*-methylbenzothiazole-2-thione (90 mg, 0.5 mmol) dissolved in a small amount (~20 mL) of methanol was added and the new reaction mixture was stirred for additional two hours at 50 °C. Slow evaporation of the clear solution at ambient afforded a pale yellow microcrystalline solid, which was filtered off and dried *in vacuo*.

2.3.1. [CuBr(xantphos)(mbtt)] (**1**)

Pale yellow crystals (199 mg, 44%), m.p. 277 °C; *Anal.* Calc. for C₄₇H₃₉NOP₂S₂CuBr: C, 62.49; H, 4.35; N, 1.55. Found: C, 62.16; H, 4.23; N, 1.48%. IR (cm^{−1}): 3047m, 2954w, 1568m, 1479s, 1456s, 1434vs, 1403vs, 1346vs, 1315s, 1286vs, 1229vs, 1136s, 1097vs, 974s, 879s, 756vs, 741vs, 701vs, 691vs, 576vs, 510vs, 464s. UV–Vis (λ_{max} , log ϵ): 239 (4.97), 275 (4.74), 322 (4.85).

2.3.2. [CuI(xantphos)(mbtt)]·CH₃CN (**2**)

Pale yellow crystals (203 mg, 41%), m.p. 234 °C; *Anal.* Calc. for C₄₉H₄₂N₂OP₂S₂CuI: C, 59.36; H, 4.27; N, 2.83. Found: C, 59.46; H, 4.22; N, 2.86%. IR (cm^{−1}): 3048m, 2968w, 1568m, 1480s, 1460s, 1432vs, 1404vs, 1350vs, 1312s, 1261s, 1226vs, 1140s, 1097vs, 979s, 875m, 755vs, 745vs, 698vs, 574vs, 510vs, 462s. UV–Vis (λ_{max} , log ϵ): 242 (5.17), 277 (4.82), 320 (5.03).

2.4. Materials and methods for biological tests

2.4.1. Materials

Agarose was purchased from BRL. Tryptone and yeast extract were purchased from Oxoid (Unipath Ltd., Hampshire, UK). All other chemicals were obtained from Sigma. Nucleic acids: Native DNA (dsDNA) type I, highly polymerized from calf thymus gland was purchased from Sigma (D-1501). The intercalative dye ethidium bromide (EthBr), were purchased from Sigma. Experiments were carried out in 50 mM Tris–Cl pH 7.5 buffer solutions to control the acidity of the reaction systems. All plastics and glassware

Table 1Crystal data and structure refinements for [CuBr(xantphos)(mbtt)] (1) and [CuI(xantphos)(mbtt)]·CH₃CN (2).

	1	2
Molecular formula	C ₄₇ H ₃₉ Br ₁ Cu ₁ N ₁ O ₁ P ₂ S ₂	C ₄₉ H ₄₂ Cu ₁ I ₁ N ₂ O ₁ P ₂ S ₂
Formula weight	903.36	991.41
T (K)	295	203
λ (Å)	0.71073	0.71073
Crystal system	triclinic	monoclinic
Space group	P-1	P2 ₁ /n
a (Å)	10.2668 (15)	10.435 (3)
b (Å)	10.6685 (9)	21.442 (6)
c (Å)	20.5421 (17)	19.939 (5)
α (°)	90.107	90
β (°)	100.076 (5)	94.079 (17)
γ (°)	110.849 (5)	90
V (Å ³)	2065.2 (4)	4450 (2)
Z	2	4
D _{calc} (Mg m ⁻³)	1.45	1.48
Absorption coefficient (μ) (mm ⁻¹)	1.712	1.389
F(000)	924	2008
Crystal size (mm)	0.06 × 0.15 × 0.34	0.07 × 0.11 × 0.19
Theta range for data collection	1.009–28.337°	1.396–26.703°
Index ranges	–13 ≤ h ≤ 12, –14 ≤ k ≤ 14, –24 ≤ l ≤ 27	–13 ≤ h ≤ 13, –25 ≤ k ≤ 26, –24 ≤ l ≤ 24
Reflections collected	32800	51923
Independent reflections (R_{int})	10221 (0.0403)	9245 (0.0834)
Completeness	99.6% ($\theta = 27.77^\circ$)	99.7% ($\theta = 25.902^\circ$)
Data/restraints/parameters	5658/0/496	5285/0/523
Refinement method	full-matrix l.s. on F^2	full-matrix l.s. on F^2
Goodness-of-fit (GOF) on F^2	1.013	1.000
Final R indices [$I > 2\sigma(I)$]	$R_1 = 0.0320$, $wR_2 = 0.0568$	$R_1 = 0.0419$, $wR_2 = 0.0884$
R indices (all data)	$R_1 = 0.0588$, $wR_2 = 0.0653$	$R_1 = 0.1087$, $wR_2 = 0.1588$
Final weighting scheme	calc $w = w' \times [1 - (\Delta F_{obs}/6 \times \Delta F_{est})^2]$ where $w' = [P_0 T_0(x) + P_1 T_1(x) + \dots + P_{n-1} T_{n-1}(x)]^{-1}$ ^a	calc $w = (1/4F_{obs}^2) \times 1$
Largest difference in peak and hole	0.33 e Å ⁻³ , –0.31 Å ⁻³	0.71 e Å ⁻³ , –0.48 Å ⁻³

^a Where P_i are the coefficients of a Chebychev series in $t_i(x)$, and $x = F_{calc}^2/F_{calc}^2_{max}$. $P_0 - P_{n-1} = 1.44 \ 1.61 \ 0.486$.

used in the biological experiments were autoclaved for 30 min at 120 °C and 130 kPa. Heat-resistant solutions were similarly treated, while heat-sensitive reagents were sterilized by filter.

The DNA stock solution (1 mg/ml) was prepared at 0–4 °C by dissolving the commercially purchased calf thymus DNA in buffer A [50 mM Tris [(hydroxymethyl)aminomethane]–HCl buffer (pH 7.5)] as solvent. Stock solutions of the complexes were prepared at a final concentration of 5 mM by dissolving the complexes in 5% DMSO–water.

2.4.2. DNA binding/cleavage experiments in agarose gel electrophoresis

The cleavage/binding reaction of DNA with metal complexes was monitored using agarose gel electrophoresis. The DNA cleavage/binding efficiency of the complexes was estimated by determining the degree of retardation/or acceleration (precedence of the electrophoretic mobility reflected in an up-shift or down-shift of the DNA to higher/or lower molecular weight DNA products, respectively). Samples, which contained aliquots of 3 μ g of the nucleic acid (DNA), were incubated at a constant temperature of 37 °C for 60 min (or as indicated in the legends) in the presence of each compound in a buffer A to a final volume of 20 μ l. It was terminated by the addition of 4 μ l loading buffer consisting of 0.25% bromophenol blue, 0.25% xylene cyanol FF (acid blue 147) and 30% glycerol in water. The products resulting from interactions of the metal complexes with DNA were separated by electrophoresis on agarose gels (1% w/v), which contained 1 μ g/ml ethidium bromide in 40×10^{-3} M Tris acetate, pH 7.5, 2×10^{-2} M sodium acetate, 2×10^{-3} M Na₂EDTA, at 5 V/cm. Agarose gel electrophoresis was performed in a horizontal gel apparatus (Mini-SubTM DNA Cell, BioRad) for about 2 h. The gels were visualized after staining with the fluorescence intercalated dye ethidium bromide under a UV

illuminator which forms a fluorescent complex when it binds to DNA.

2.4.3. Determination of antimicrobial activity by the well-diffusion method

Antimicrobial activities of the newly synthesized complexes were determined using Gram-negative bacteria (*Escherichia coli* and *Xanthomonas campestris*) and Gram-positive bacteria (*Bacillus subtilis* and *Bacillus cereus*) following a modified Kirby Bauer disc diffusion method [26,27]. In brief, the bacteria were cultured in LB Broth at 37 °C on a shaking incubator at 130 rpm. A lawn of bacterial culture was prepared by spreading 100 μ l culture broth, having 10^6 CFU/ml of each test organism on solid nutrient agar plates. The plates were allowed to stand for 10–15 min to allow for culture absorption. The 8 mm size wells were punched into the agar with the head of sterile micropipette tips. Using a micropipette, 5, 10 and 15 μ l of the complexes were poured into each of five wells on all plates. After incubation at 37 °C for 24 h, the size of the zone of inhibition was measured. A volume of 15 μ l of culture medium was run as a negative control whereas the same volume from a solution (100 mg/ml) of the antibiotic ampicillin was used as a positive control.

2.4.4. Lipid peroxidation measurement

During the lipid peroxidation (a major indicator of oxidative stress) of unsaturated fatty acid by oxygen based free radicals, the malondialdehyde (MDA) is produced and the measured intensity is related to the concentration of generated reactive oxygen species (ROS). In a biological system, ROS is determined by using the thiobarbituric acid reactive species (TBARS) method, which is based on the quantification of a pink colored complex between thiobarbituric acid and malondialdehyde (MDA) after acid

hydrolysis reaction that can be quantitatively measured on a spectrophotometer at $\lambda_{\text{max}} = 532 \text{ nm}$ [28–30]. Briefly, *E. coli* cells were initially cultivated on LB medium for 24 h at 37 °C and then were collected when culture reached exponential or stationary phase. Cells were suspended in buffer A and aliquots containing 50 mg cells were transferred in each tube. Exponential or stationary bacterial cells (50 mg) were directly exposed to 10 mM hydrogen peroxide (H_2O_2) or to increasing concentrations of each of the complexes **1** and **2** for 1 h at 37 °C. Then cells were harvested by centrifugation and washed twice with distilled water. The pellets were re-suspended in 500 μL of a 10% trichloroacetic acid (TCA) solution and transferred to a tube containing 1.5 g of glass beads. Cells were lysed by 15 cycles of agitation in a vortex for 20 s and incubated on ice for 20 s, followed by 30 cycles of sonication at 225 W for 10 s and 10 s incubation on ice. The supernatants obtained after centrifugation were mixed with 0.1 mL of 0.1 M EDTA, 0.6 mL of 0.1% w/v thiobarbituric acid in 0.05 M NaOH. The reaction mixture was incubated at 100 °C for 15 min. The samples were cooled, centrifuged (5900 g) for 5 min, and the appearance of MDA was recorded by measuring in the supernatant the absorbance at 532 nm and compared to a standard curve containing 0–3.2 μM MDA.

3. Results and discussion

3.1. Preparative considerations

The preference of a rigid bidentate ligand for a certain coordination mode (chelating or bridging) depends, to a significant degree, on its “bite angle”, and chelation is normally favoured for bite angles close to those required by the geometry of the coordination polyhedron being formed. The structural motifs usually adopted by copper(I) halide complexes bearing chelating rigid diphosphanes in a tetrahedral coordination environment are either discrete monomers, or dimers containing the $\text{M}(\mu_2\text{-X})_2\text{M}$ core [31,32]. Consequently, the ability of such diphosphanes to span tetrahedral sites under formation of fairly constrained P–M–P angles having values far away from their quite short natural bite angles, should be connected with the extraordinary versatility of the d^{10} metal ion. In this respect, the potentiality of xantphos to chelate copper(I), either in a tetrahedral or in a trigonal planar environment can be easily explained, while steric demands on the part of the ligands may be responsible for the adoption of a distinct coordination number in each case. Indeed, treatment of CuX with xantphos, independent of the ratios of the phosphane applied, results in the formation of a three-coordinate chelate, whereas subsequent addition of one equivalent of a heterocyclic thione to the solution of $[\text{CuX}(\text{xantphos})]$ causes increase of the coordination number, leading to the formation of four-coordinate xantphos/thione mixed-ligand species. This was once again the case with the reactions within the present study, where the favored four-coordination for copper(I) could be easily achieved even using the more bulky ligand *N*-methylbenzothiazole-2-thione.

The microcrystalline solids are moderately soluble in acetonitrile, dichloromethane and chloroform and only slightly soluble in acetone. Their solutions in acetonitrile are stable to air and moisture and exhibit no conductivity. Room temperature magnetic measurements confirm the expected diamagnetic nature of the compounds.

3.2. Spectroscopy

The electronic absorption spectra of the two complexes, recorded in acetonitrile at room temperature, show three intense broad bands with maxima in the ~ 240 , ~ 276 and $\sim 321 \text{ nm}$

regions. Although exact assignment of the two high energy bands is difficult since both the *N*-methylbenzothiazole-2-thione and xantphos strongly absorb in the same regions, with reference to the absorption spectrum of the uncoordinated xantphos, these bands can be considered as intraligand $\pi^* \leftarrow \pi$ transitions on the phenyl groups of both the phosphane and the thione moiety and as a phosphane-originating MLCT transition, respectively. The lower energy band can be attributed to a thione originating CT transition at the C=S bond which may possess some MLCT character [33,34].

The solid state FT-IR spectra recorded in the range 4000–250 cm^{-1} show all the expected strong phosphane bands, which remain practically unshifted upon coordination. Moreover, they contain the characteristic bands required by the presence of the *N*-methylbenzothiazole-2-thione ligand. In particular, the intense bands at 1411 and 1259 cm^{-1} in the spectrum of free mbtt, attributed to the C–N stretching vibration, appear in the spectra of all complexes slightly shifted to higher energies, indicating an exclusive S-coordination of the ligand. On the other hand, the strong band at 1095 cm^{-1} assigned to the C=S stretching [35], remains essentially unshifted upon coordination, being hereby less informative with regard to the ligand's coordination mode.

3.3. Description of the structures

The X-ray crystal structures of $[\text{CuBr}(\text{xantphos})(\text{mbtt})]$ (**1**) and $[\text{CuI}(\text{xantphos})(\text{mbtt})]$ (**2**) (details of crystal and structure refinement are shown in Table 1) have been determined. Pale yellow crystals of both **1** and **2** were grown from their respective acetonitrile/methanol mother liquid upon slow evaporation during several days. Compound **1** crystallizes in the triclinic system $\bar{P}1$, with two discrete molecules in the unit cell, while **2** crystallizes in the monoclinic space group $P2_1/n$, with four discrete formula units and four lattice CH_3CN molecules in the unit cell. Tables 2 and 3 list selected distances and angles of these complexes, and perspective drawings showing the atom numbering are shown in Figs. 1 and 2.

The two structures are similar having common the tetrahedral coordination of the copper(I) center, which is surrounded by the S donor of the thione ligand, two P atoms of the chelating xantphos unit, as well as the corresponding halogen atom. In compound **1**, angular deviations from the ideal tetrahedral value of 109.4° are quite small, thus the tetrahedral environment of the copper atom can be considered as essentially regular when compared with several reported, four coordinated, copper(I) halide complexes bearing a heterocyclic thione and two monodentate arylphosphanes or a chelating short bite angle diphosphane [31]. Contrary to that, the $\text{I}(1)\text{--Cu}(1)\text{--S}(1)$ and $\text{S}(1)\text{--Cu}(1)\text{--P}(1)$ angles in **2**, having values of 92.11(5)° and 119.44(7)°, respectively, deviate remarkably from the ideal tetrahedral expectation. While the $\text{P}(1)\text{--Cu}(1)\text{--P}(2)$ angles of 111.52(3)° in **1** and 113.85(6)° in **2** are very close to the ligands calculated “natural” bite angle of 111° [36], it is obvious that chelation requires some adjustment on the part of the diphosphane backbone, to keep constraints within the tetrahedron at a minimum. In fact, the P...P distance of 4.045(1) Å of the xanthene unit appears shortened to values of 3.799 and 3.832 Å in **1** and **2**, respectively, accompanied by a respective adaptation of the folding of the molecule along the axis through the oxygen atom and the xanthene carbon atom C(45) (141.60° in **1** and 139.55° in **2** versus 156.58° in the free xantphos [37]).

In both structures, the two individual Cu–P distances are within the limits of the range expected for tetrahedrally coordinated copper(I). Likewise, the Cu–S and Cu–Br and Cu–I bond lengths are comparable to those reported for other tetrahedrally coordinated copper(I) complexes with terminal bromine or iodine and thione-sulfur donors [18,38].

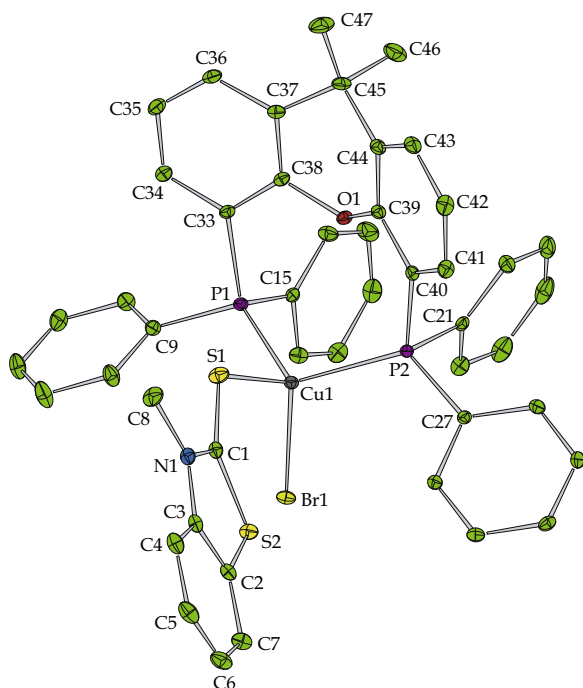
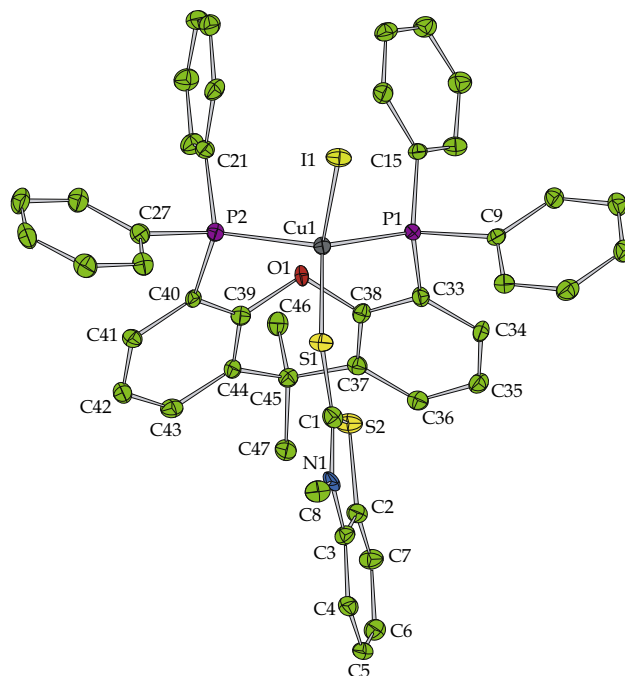
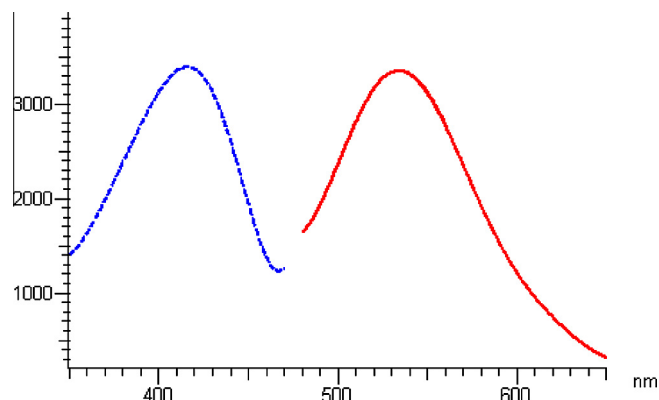
Table 2

Selected bond distances (Å) and angles (°) in [CuBr(xantphos)(mbtt)] (1).

Cu(1)–Br(1)	2.4468(6)	Br(1)–Cu(1)–S(1)	114.85(3)
Cu(1)–S(1)	2.3797(10)	Br(1)–Cu(1)–P(1)	103.52(3)
Cu(1)–P(1)	2.3019(9)	Br(1)–Cu(1)–P(2)	111.66(3)
Cu(1)–P(2)	2.2947(9)	S(1)–Cu(1)–P(1)	105.17(4)
S(1)–C(1)	1.671(3)	S(1)–Cu(1)–P(2)	109.79(4)
		P(1)–Cu(1)–P(2)	111.52(3)

Table 3Selected bond distances (Å) and angles (°) in [CuI(xantphos)(mbtt)]·CH₃CN (2).

Cu(1)–I(1)	2.6570(9)	I(1)–Cu(1)–S(1)	92.11(5)
Cu(1)–S(1)	2.3543(19)	I(1)–Cu(1)–P(1)	108.58(5)
Cu(1)–P(1)	2.2897(17)	I(1)–Cu(1)–P(2)	110.59(4)
Cu(1)–P(2)	2.2825(17)	S(1)–Cu(1)–P(1)	119.44(7)
S(1)–C(1)	1.650(7)	S(1)–Cu(1)–P(2)	110.04(7)
		P(1)–Cu(1)–P(2)	113.85(6)

**Fig. 1.** Molecular plot of [CuBr(xantphos)(mbtt)].**Fig. 2.** Molecular plot of [CuI(xantphos)(mbtt)].**Fig. 3.** Room-temperature solid-state excitation (dashed line, $\lambda_{\text{em}} = 534$ nm) and emission (solid line, $\lambda_{\text{ex}} = 410$ nm) spectrum of [CuBr(xantphos)(mbtt)] (1).

3.4. Photoluminescence

Room-temperature photoexcitation of solid samples of each of the two compounds under consideration at $\lambda = 410$ nm produces an intense broad emission band with peak maximum at $\lambda = 534$ and 532 nm for **1** and **2**, respectively (Fig. 3). This emission cannot be considered as one of pure intra-ligand origin, because of its significant red shift relative to the solid-state r.t. emission spectrum of the free xantphos, which consists of a broad band centered around 465 nm, being more compatible with a metal-to-ligand charge-transfer ($\text{Cu} \rightarrow \pi^*(\text{xantphos})$) excited state, mixed with IL ($\pi \rightarrow \pi^*$) transitions associated with the phenyl rings of xantphos. Contrary to our previous results from related compounds [39–41], no significant shift of the emission energy is observed upon changing of the halide ligand, thus the participation of a halide-to-ligand charge-transfer (XLCT) in the emissive excited sites seems here unlikely.

3.5. Evaluation of biological activity

3.5.1. DNA binding/cleavage experiments in agarose gel electrophoresis

The effect of the two newly synthesized copper complexes on the integrity of calf thymus ds DNA (CTDNA) was examined.

When ds CT-DNA was treated with low concentrations (0.5 and 1 mM) of both compounds **1** and **2** the integrity seemed to be unaffected visibly in both cases (Fig. 4A). However, when CT-DNA was treated with a concentration of 2 mM of compound **1** significant degradation was caused, as it is deduced from the diminution of the initial amount of CTDNA (Fig. 4B, lane 2). In addition, at a higher concentration of 3 mM the ds CT-DNA was completely degraded (Fig. 4B, lane 3) ending in the disappearance of the main DNA band. In contrast, the integrity of ds CT-DNA remained unaffected after treatment with compound **2** or with each of the ligands (mbtt or xantphos) under the same conditions.

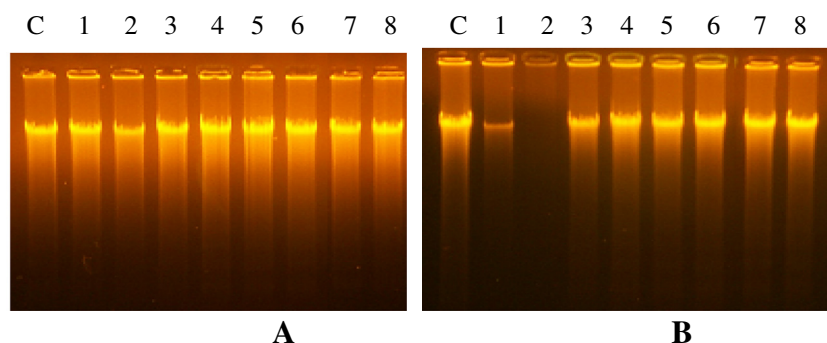


Fig. 4. Dose dependent DNA degradation action of compounds **1** and **2** and the free ligand xanthos and separation in agarose (1%) gel electrophoresis of ds CTDNA. Each sample containing 3 μ g of ds CTDNA was treated with 0.5 mM and 1 mM of compounds **1**, **2** and xanthos. (A) Lane C: control, Lanes 1–2: 0.5 and 1 mM of compound **1**, respectively. Lanes 3–4: 0.5 and 1 mM of compound **2**, respectively. Lanes 5–6: 0.5 and 1 mM of xanthos, respectively. Lanes 7–8: 0.5 and 1 mM of mbtt, respectively. (B) Lane C: control, Lane 1–2: 2 and 3 mM of compound **1**, respectively. Lanes 3–4: 2 and 3 mM of compound **2**, Lanes 5–6: 2 and 3 mM of xanthos, respectively. Lanes 7–8: 0.5 and 1 mM of mbtt, respectively.

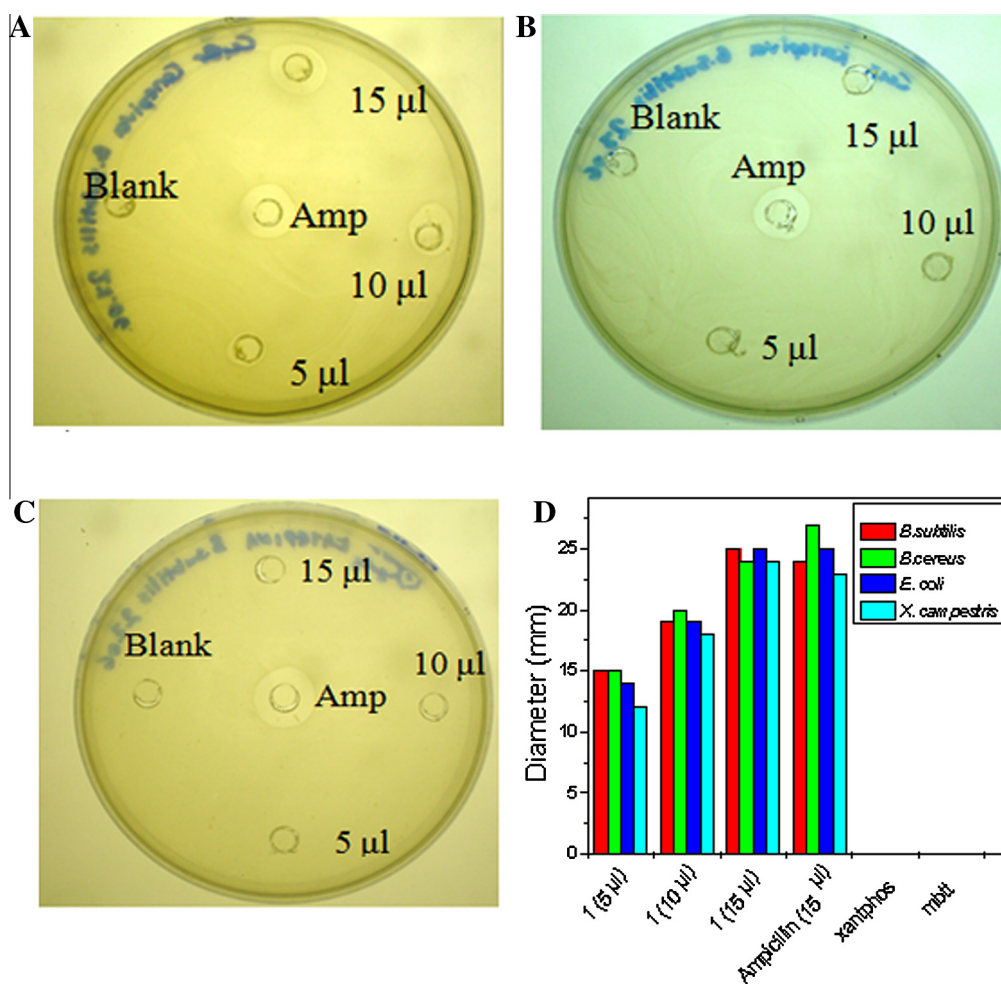


Fig. 5. Zones of inhibition of copper complexes in representative agarose plates against *B. subtilis*, of the antibiotic ampicillin (100 mg/ml) as a positive control and of culture medium as a negative control (blank). Plates A–C: A volume of 5, 10 and 15 μ l of a 3 mM solution of compounds **1** and **2** and the free ligand xanthos were spotted in each well of the plates, wherein the bacterium *B. subtilis* was incorporated. (D) Bar graph representing the zone of inhibition for compounds **1** and **2** and their ligands compared to the antimicrobial activity exhibited from 15 μ l of a solution of ampicillin (100 mg/ml) against *B. subtilis*, which was considered as 100%.

3.5.2. Determination of antimicrobial activity by the well-diffusion method

The antimicrobial activities were determined against two Gram-negative (*E. coli* and *X. campestris*) and two Gram-positive bacteria (*B. subtilis* and *B. cereus*) following a modified Kirby Bauer well-diffusion method.

Fig. 5 shows representative images exhibiting the zone of inhibition caused by each of the two copper complexes as well as the free ligands at three different volumes (5, 10 and 15 μ l) from their solutions at concentration 3 mM. In the center of each plate a volume of 15 μ l of a 100 mg/ml solution of the known antibiotic ampicillin was spotted and the zone of inhibition was recorded,

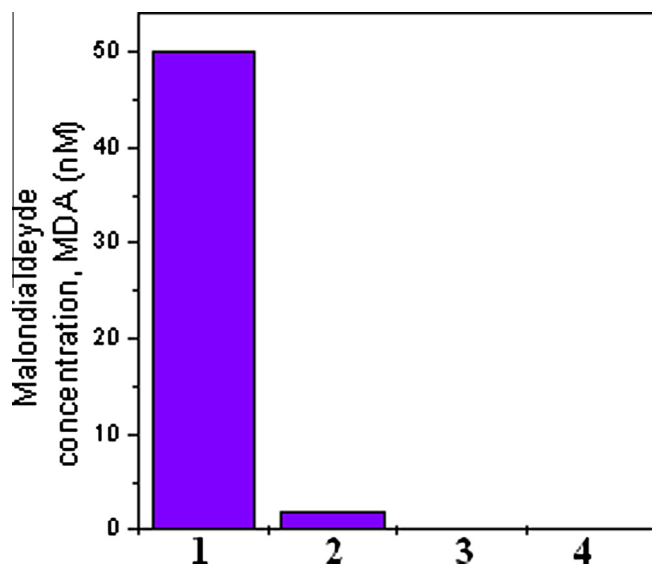


Fig. 6. Increase in the MDA equivalents (nmol/ml) with exposition to (1) 3 mM compound 1, (2) 3 mM of compound 2, (3) 3 mM of xantphos and (4) 3 mM of mbtt.

as a positive control. It should be noted that the concentration of this ampicillin solution (molecular mass = 349.41) was about hundred times higher than the concentration used for each of the compounds under investigation. In addition, the culture media alone was spotted and its antimicrobial activity was recorded as a negative control.

As it is obvious, among the compounds tested only compound 1 clearly inhibits the growth of both Gram-negative and -positive bacteria and, in addition, the zone of inhibition increases with the increase of the complexes amount. Moreover, it can be seen that the same volume of a solution of compound 1 (2.71 mg/ml) proves to be as effective as the about hundred times more concentrated solution of the antibiotic ampicillin (100 mg/ml), producing the same zones of inhibition against the bacterium *B. subtilis* under the same conditions. Similar results were obtained with all other bacteria tested.

3.5.3. Lipid peroxidation measurement

The oxidation of cell membrane lipids could be triggered by reactive oxygen species like H_2O_2 or highly reactive hydroxyl radical and singlet oxygen, which were often reported to be generated by toxic agents. The toxicity of the newly synthesized Cu complexes was studied in *E. coli* also in the light of formation of reactive oxygen species (ROS), measured as malondialdehyde (MDA) equivalent by thiobarbituric acid-ROS (TBARS) assay. Higher inhibition of growth for the chronic exposure batches were correlated with higher ROS generation, which subsequently contributed to cause membrane lipid peroxidation.

Compared to the control batch (i.e., without complexes or ligands in culture media), the MDA equivalents for the cells treated with compound 1 were higher than the MDA equivalents for the cells treated with compound 2 and for the cells treated with xantphos (Fig. 6). Neither compound 2 nor the ligand xantphos seems to create any MDA equivalents. *E. coli* cells produce approximately 50 nM malondialdehyde (MDA) after one hour of exposition to compound 1, which can be attributed to lipid peroxidation. Similar results were obtained with the other bacteria. It should be noted that for *E. coli* cells that were not exposed in any agent, the MDA equivalents were not detectable (sample of reference).

4. Conclusion

The aim of this work was the preparation, characterization and the study of the antibacterial activity of copper(I) halide mixed-ligand complexes bearing *N*-methylbenzothiazole-2-thione bonded to the metal via the thione-S atom and 4,5-bis(diphenylphosphano)-9,9-dimethylxanthene as a chelating ligand. According to the overall geometries of the two structures presented here, the xantphos ligand applied can be considered as best tailored for chelation of copper(I) centres, as it seems not to be forced, upon coordination, to significantly modify its natural bite angle. The new compounds show intense room temperature luminescence in the solid state, most likely originating from emissive excited states of mixed MLCT/IL character.

Remarkably high antimicrobial activity, significantly higher than that of the commercially available antibiotic ampicillin against some Gram-negative and Gram-positive bacteria is found only for the copper bromide complex (compound 1) unlike its iodide counterpart which is found to be quite inactive. This antibacterial activity is mediated by the generation of ROS and damage of bacterial membrane. Likewise DNA degradation to a significant degree upon interaction with CT-DNA is observed only for the copper bromide complex. This different behavior is a rather strange finding and requires to be further investigated.

Acknowledgments

This research has been co-financed by the European Union (European Social Fund – ESF) and Greek national funds through the Operational Program “Education and Lifelong Learning” of the National Strategic Reference Framework (NSRF) – Research Funding Program: ARCHIMEDES III. Investing in knowledge society through the European Social Fund.

Appendix A. Supplementary data

CCDC 972048 and 972049 contain the supplementary crystallographic data for compounds 1 and 2, respectively. These data can be obtained free of charge via <http://www.ccdc.cam.ac.uk/conts/retrieving.html>, or from the Cambridge Crystallographic Data Centre, 12 Union Road, Cambridge CB2 1EZ, UK; fax: +44 1223-336-033; or e-mail: deposit@ccdc.cam.ac.uk.

References

- [1] R.J. Puddephatt, Chem. Soc. Rev. 12 (1983) 99.
- [2] F.A. Cotton, K.R. Dunbar, M.G. Verbruggen, J. Am. Chem. Soc. 109 (1987) 5498.
- [3] R.V. Kireess, R. Eisenberg, Inorg. Chem. 28 (1989) 3372.
- [4] S.J. Bernes-Price, R.K. Johnson, C.K. Mirabelli, L.F. Faucette, F.L. McCabe, P.J. Sadler, Inorg. Chem. 26 (1987) 3383, and references therein.
- [5] R.H. Holm, P. Kennepohl, E.I. Solomon, Chem. Rev. 96 (1996) 2239.
- [6] J.A. Garcia-Vazquez, J. Romero, A. Sousa, Coord. Chem. Rev. 193–195 (1999) 691, and references therein.
- [7] P.D. Akrivos, Coord. Chem. Rev. 213 (2001) 181.
- [8] B.A. Al-Maythallony, M. Monim-ul-Mehboob, M. Altaf, M.I.M. Wazeer, A.A. Isab, S. Altuwajjri, A. Ahmed, V. Dhuna, G. Bhatia, K. Dhuna, S. Singh Kamboj, Spectrochim. Acta, Part A 115 (2013) 641.
- [9] S. Braun, A. Botzki, S. Salmen, C. Textor, G. Bernhardt, S. Dove, A. Buschauer, Eur. J. Med. Chem. 46 (2011) 4419.
- [10] C. Congiu, M.T. Cocco, V. Omnis, Bioorg. Med. Chem. Lett. 18 (2008) 989.
- [11] M.S. Masoud, A.A. Soayed, A.F. El-Husseiny, Spectrochim. Acta, Part A 99 (2012) 365.
- [12] Y. Liu, J. Wu, P.-Y. Ho, L.-C. Chen, C.-T. Chen, Y.-C. Liang, C.-K. Cheng, W.-S. Lee, Cancer Lett. 271 (2008) 294.
- [13] C.-R. Shih, J. Wu, Y. Liu, Y.-C. Liang, S.-Y. Lin, M.-T. Sheu, W.-S. Lee, Biochem. Pharmacol. 67 (2004) 67.
- [14] P. Aslanidis, P.J. Cox, P. Karagiannidis, S.K. Hadjikakou, C.D. Antoniadis, Eur. J. Inorg. Chem. (2002) 2216, and references therein.
- [15] M.A. Tsiaggali, E.G. Andreadou, A.G. Hatzidimitriou, A.A. Pantazaki, P. Aslanidis, J. Inorg. Biochem. 121 (2013) 121.
- [16] M. Porchia, F. Benetollo, F. Refosco, F. Tisato, C. Marzano, V. Gandin, J. Inorg. Biochem. 103 (2009) 1644.

- [17] C. Marzano, M. Pellei, S. Alidori, A. Brossa, G.G. Lobbia, F. Tisato, C. Santini, J. Inorg. Biochem. 100 (2006) 299.
- [18] A. Kaltzoglou, P.J. Cox, P. Aslanidis, Inorg. Chim. Acta 358 (2005) 3048.
- [19] A. Kaltzoglou, P.J. Cox, P. Aslanidis, Polyhedron 26 (2007) 1634.
- [20] G. Storz, J.A. Imlay, Curr. Opin. Microbiol. 2 (1999) 188.
- [21] J.A. Imlay, Annu. Rev. Microbiol. 57 (2003) 395.
- [22] Bruker Analytical X-ray Systems, Inc. Apex2, Version 2 User Manual, M86-E01078, Madison, WI, 2006.
- [23] L. Palatinus, G. Chapuis, J. Appl. Crystallogr. 40 (2007) 786.
- [24] P.W. Betteridge, J.R. Carruthers, R.I. Cooper, K. Prout, D.J. Watkin, J. Appl. Crystallogr. 36 (2003) 1487.
- [25] D.W. Watkin, C.K. Prout, L.J. Pearce, CAMERON, Chemical Crystallography Laboratory, Oxford, UK, 1996.
- [26] A.W. Bauer, W.M. Kirby, J.C. Sherris, M. Turck, Am. J. Clin. Pathol. 45 (1966) 493.
- [27] A. Azam, A.S. Ahmed, M. Oves, M.S. Khan, A. Memic, Int. J. Nanomed. 7 (2012) 3527.
- [28] E.L. Steels, R.P. Learmonth, K. Watson, Microbiology 140 (1994) 569.
- [29] L.T. Rael, G.W. Thomas, M.L. Craun, C.G. Curtis, R. Bar-Or, D. Bar-Or, J. Biochem. Mol. Biol. 37 (2004) 749.
- [30] G.J. Pacheco, R.S. Reis, A.C. Fernandes, S.L. da Rocha, M.D. Pereira, J. Perales, D.M. Freire, Appl. Microbiol. Biotechnol. 95 (2012) 1519.
- [31] P. Aslanidis, P.J. Cox, S. Divanidis, P. Karagiannidis, Inorg. Chim. Acta 357 (2004) 1063.
- [32] P. Aslanidis, P.J. Cox, A. Kaltzoglou, A.C. Tsipis, Eur. J. Inorg. Chem. (2006) 334.
- [33] A.A. Del Paggio, D.R. McMillin, Inorg. Chem. 22 (1983) 691.
- [34] C. Kutal, Coord. Chem. Rev. 99 (1990) 213.
- [35] F. Cristiani, F.A. Devillanova, G. Verani, Spectrochim. Acta 12 (1982) 1299.
- [36] S. Hillebrand, J. Bruckmann, C. Krüger, M.W. Haenel, Tetrahedron Lett. 36 (1995) 75.
- [37] M. Kranenburg, Y.E.M. van der Burg, P.C.J. Kamer, P.W.N.M. Leeuwen, J. Fraanje, Organometallics 14 (1995) 308.
- [38] P.J. Cox, A. Kaltzoglou, P. Aslanidis, Inorg. Chim. Acta 359 (2006) 3183.
- [39] P. Aslanidis, P.J. Cox, P. Tsaliki, Polyhedron 27 (2008) 3029.
- [40] P. Aslanidis, P.J. Cox, A.C. Tsipis, Dalton Trans. 39 (2010) 10238.
- [41] I. Papazoglou, P.J. Cox, A.G. Papadopoulos, M.P. Sigalas, P. Aslanidis, Dalton Trans. 42 (2013) 2755.